Advanced Materials Research Vols. 133-134 (2010) pp 1195-1200
© (2010) Trans Tech Publications, Switzerland
doi:10.4028/www.scientific.net/AMR.133-134.1195

Experimental Studies of Reinforced Concrete Column Capacity Affected by Core Drilling

ZHU Lei[1,a], XU Qingfeng[1,b], LI Xiangmin[2,c] and ZHU Chunming[2,d]

[1] Shanghai Key Laboratory of New Technology Research on Engineering Structure, Shanghai, China

[2] Shanghai Research Institute of Building Sciences, Shanghai, China

[a]zhulei@sribs.jk.sh.cn, [b]qingfengxu@yahoo.com.cn, [c]lxm_sh@tom.com, [d]zhucm@online.sh.cn

Abstract: The paper presents the experimental studies of reinforced concrete column (RC column) capacity affected by core drilling. By testing three groups (9 total) of full scale concrete short columns, the experiment demonstrates that the axial compression capacity of RC columns after core drilling is reduced from 5.63% to 22.14% while the ultimate displacement decreases from 1.88% to 26.14%. The behavior of columns is altered from the axial compression failure to a small-eccentricity compression failure. The paper summarizes experiment results, followed by an investigation of the dominant factors, such as column effective cross section, drilling location, drilled hole repairing and reinforcing steels discontinued by drilling, that have impact on RC column capacity. The rationale of capacity variations of RC columns due to core drilling is also investigated.

Key words: RC column, core drilling, capacity, experimental study

Introduction

The core drilling is one of the partially destructive tests to determine concrete strength of RC members. The technique has appeared in engineering applications since 1981 in China (CECS 03:88 1988). Although it would introduce a localized damage, core drilling test provides the excellence of easy inspection, precise examination, and broad application as compared to other concrete testing techniques. Core drilling has become an effective method of concrete strength determination and gained extensive applications in the field of building structure appraisal and rehabilitation as well as analyses and treatment of engineering failure.

With the increasing demand of sustainable development and environmental-friendly, China has been enhancing efforts in utilization and rehabilitation of existing buildings especially those with historic architecture value. This requires an method that can precisely test and assess the concrete strength of existing structures. Core drilling test is so far a reliable method to accurately determine concrete strength. Concrete strength determination by concrete drilled cores has been studied by some researchers (Bungey J 1979, Bartlett M and MacGregor J (1994a, 1994b, 1994c)). However, the impact of drilled-hole on the axial capacity of concrete structural members is still lack of studies. The usage of core drilling test method shall take into account its potential negative impact on structure safety. The paper is focused on the studies of the capacity alternation and the failure configuration of RC columns by the factors of drilling location, column cross-section size and core fill after drilling.

Experiment Description

Specimen Design Total 9 full-scale RC columns are constructed and sorted into 3 groups by numbering from C1 to C9. Group 1 has 2 columns, C1 and C2 with an identical cross section of 300mm x300mm. Group 2 has 4 columns, numbered from C3 to C6, with a cross section of 400mm x 400mm. Group 3 has 3 columns, C7 to C9, with a cross section of 400mm x 600mm. All columns are 1200mm high.

The concrete mixing ratio is 132 : 267 : 856 : 1052 : 47 : 3.5 of water, cement, fine aggregate (sand), coarse aggregate (crushed stone), cementitious materials (fly ash) and chemical admixture (ZK-9011). The compressive strength of concrete is 19.5 MPa on average. Slight-expansion high-strength concrete employed for repairing drilling hole of C6 has a strength of 58.6 MPa on average, and C6 remains vertically erected while the drilled core hole is patched.

Each group of specimens has an identical rebar arrangement with a standard cover of 25mm. Key parameters of the specimens are listed in Table 1 and Fig. 1.

Table 1: Key Parameters of Specimens

Group no.	Specimen	Diemnsion (mm × mm)	Location of Core Drilling	Steel Ratio(%)	Rebar Strength		Cylinder Strength (MPa)	Drilled Core Strength (MPa)
					Yield (MPa)	Ultimate (MPa)		
1	C1	300 × 300	-	1.00	385	551	19.5	-
	C2	300 × 300	Offset Center					19.2
2	C3	400 × 400	-	1.00	367	525	19.5	-
	C4	400 × 400	Offset Center					20.7
	C5	400 × 400	Center					21.0
	C6	400 × 400	Center					18.0
3	C7	400 × 600	-	0.84	367	525	19.5	-
	C8	400 × 600	Center offset at short dim.					20.2
	C9	400 × 600	Center at long dim.					21.9

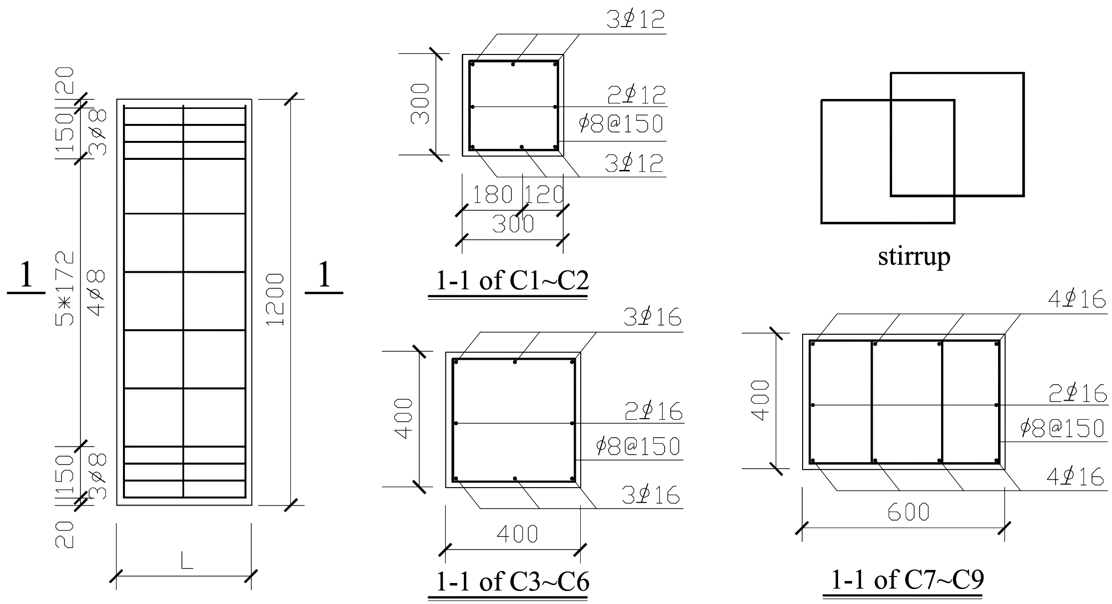

Figure 1: Dimensions and Reinforcement of Specimens

Location of Core Drilling C1, C3 and C7 are control specimen in each group. C2 has a drilled core with its center 60mm offset from the center line of column side face. In order to remain continuous, the vertical rebar in way of drilling is positioned 30mm away from the center line of the column. C4 is core drilled at the location 100mm away from the center line of column side without rebars being cut. C5 and C6 are core drilled at the center line of columns with rebars cut. However, the drilled hole of C6 is repaired by slight-expansion high-strength concrete. Core drilling is performed at 100 mm offset from the center line at the short dimension side of C8, Instead C9 has a drilled core at the center of the long dimension side. Reinforcing rebars of C8 and C9 remain continuous.

All drilled cores are located vertically in the middle of columns. Core cylinders have a diameter of 100 mm and a depth of 140 mm, leaving 110mm-diameter core holes on the columns.

Layout of Strain Gauge In order to assess the capacity impacts by drilled cores, strain gauges are deployed at vertical rebars, stirrups and concrete surface. Other than strain gauges, LVDT are also set up during the experiment. The core drilling lacation, layout of strain gauges and LVDT of C5 and C6 are shown in Fig. 2.

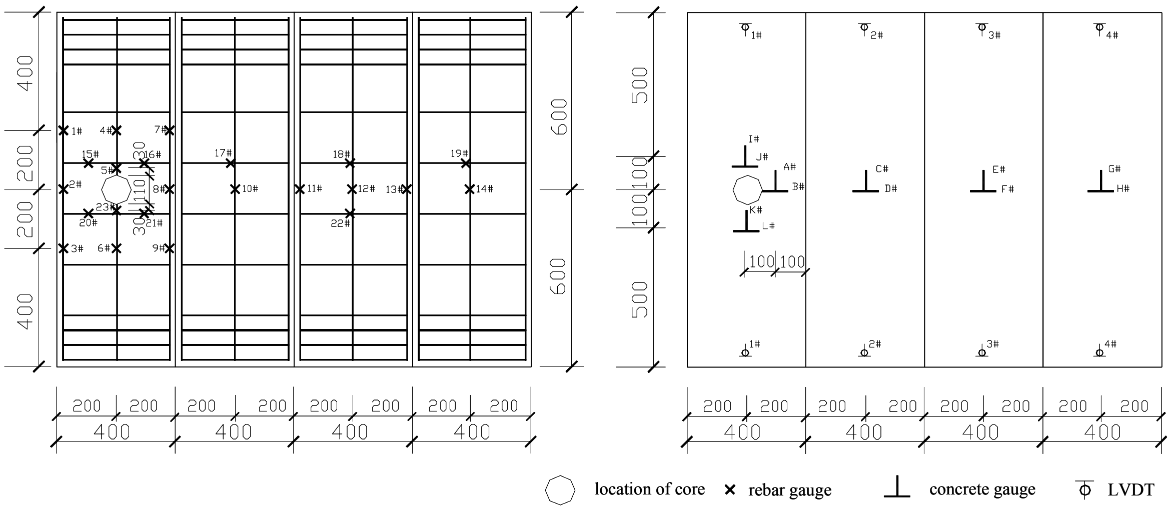

Figure 2: Core Drilling Location, Layout of Strain Gauges and LVDT of C5 and C6

Experiment Equipment and Measurements The experiment is accomplished at a 10000kN multi-function large-scale structural testing system. Experiment data are acquired by a data collection system of Solartron SI 35951B IMP. Specimens are loaded at a speed of 0.3mm/min.

Experiment Results

The main experiment results are summarized and compared in Table 2.

Table 2: Main Experiment Results

Specimen No.	Loading of Initial Cracking (kN)	Ultimate Capacity		Ultimate Displacement	
		Recorded Reading (kN)	Percentage (%)	Recorded Reading (mm)	Percentage (%)
C1	1390	1616	—	2.702	—
C2	600	1525	5.63	2.102	22.21
C3	1970	2872	—	2.445	—
C4	1700	2236	22.14	2.399	1.88
C5	1450	2448	14.76	2.330	4.70
C6	1380	2764	3.76	2.506	-2.49
C7	1900	4446	—	3.432	—
C8	1650	4031	9.33	2.535	26.14
C9	2170	4080	8.23	2.537	26.08

Characteristics of Specimen Failure C1 fails with an axial-compression mode and cracks are uniformly distributed over four sides (Fig. 3). C2 has initial vertical cracks occurring on top of the cored-hole. When approaching its ultimate capacity, C2 exhibits an asymmetrical distribution of cracks over four column sides. Concrete around the cored-hole is crushed with the rebars remaining un-yielded, which demonstrates a typical column failure subject to small-eccentricity compression.

C3 reaches its axial-compression failure, cracks on each side face are developed and distributed regularly while strains of concrete and rebars are detected evenly on each column side. C4 shows vertical cracks initially on the side with cored-hole. When proceeding to its ultimate capacity, the column displays vertical cracks most on the cored-side. The failure indicates a small-eccentricity compression failure (Fig. 4). C5 experiences a similar failing procedure as described for C4 in the failure mode of small-eccentricity compression. C6 shows vertical cracks evenly distributed over four sides. At its point of ultimate capacity, C6 has vertical cracks crossed over the core-filled concrete and fails owing to an axial compression.

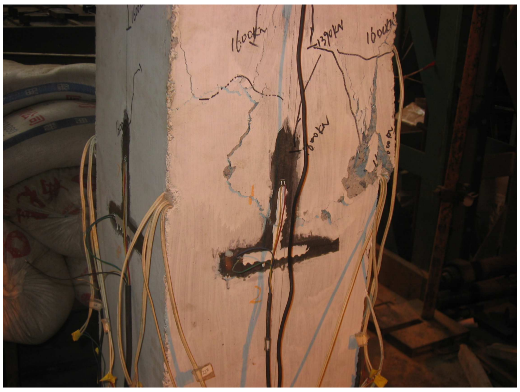

Figure 3: Axial Compression Failure of C1

Figure 4: Small-Eccentricity Compression Failure of C4

C7 firstly presents vertical cracks at the third points of the column bigger side (600 mm) and then on the center line of shorter side (400 mm). When C7 approaches to its failure, six extensive top-down cracks are established while the center portion of column concrete are crushed. C8 also first presents vertical cracks originally at third points on bigger side, and then vertical cracks are perceived firstly at the shorter side with cored-hole prior to its opposite side. When small-eccentricity compression failure achieved, both bigger sides of C8 have similar crack patterns, but vertical cracks on the cored-hole side are more adverse as compared to its opposite side. C9 shows two vertical cracks at third points of cored-hole side and one at its opposite side. Loaded at its capacity, C9 illustrates similar crack patterns on both shorter sides. Cracks on the cored-hole side are more intense than its opposite side. C9 fails with failure characteristics attributed to small-eccentricity compression.

Studies of Experiment Results The P-Δ curves of three groups of specimens are shown in Figure 5~7 respectively.

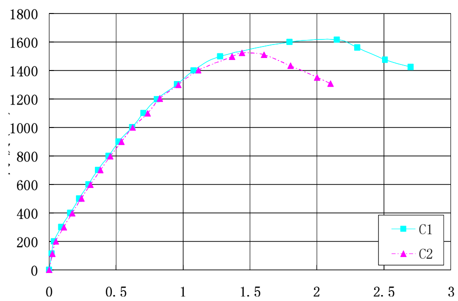

Figure 5: P-Δ Curves of Specimens C1, C2

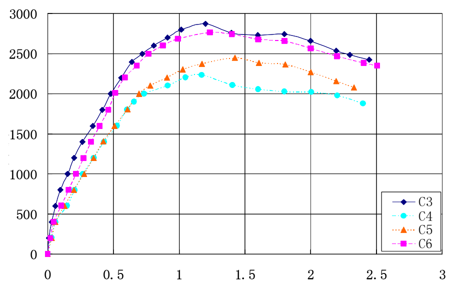

Figure 6: P-Δ Curves of Specimens C3, C4, C5, C6

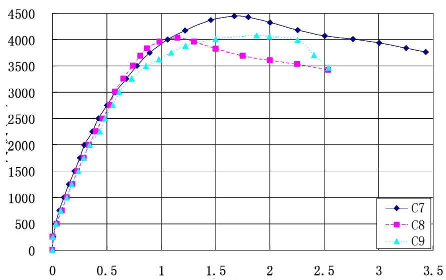

Figure 7: P-Δ Curves of Specimens C7, C8, C9

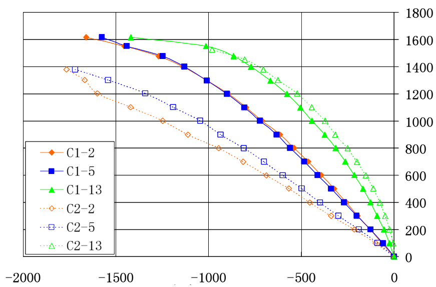

Figure 8: Rebar Strains of Specimens C1, C2

Column Ultimate Capacity and Rationale of Regression It can be noted from Table 2 that the specimens with drilled cores have lower ultimate capacities than their control specimens. A decline of column ultimate compression capacity between 5.63% and 22.14% is monitored in the experiment. But C6, the specimen which drilled hole is repaired, shows only 3.76% decline of its capacity. Derived from the P-Δ curves of three groups shown in Figure 5~7, the initial stiffness of the drilled columns is also less than that of their corresponding comparisons.

It is illustrated further in Table 2 and Figure 6 that C5, of which the drilled core is located at the center line, has a capacity decline of 14.76%. The percentage of capacity decline is less noticeably than that of C4, which capacity is reduced by 22.14%. The difference of capacity deterioration is determined by the core drilling location. The cross section of C5 is only unsymmetrical in single principal centroidal axis at the cored-hole location. However, the cross section of C4 is unsymmetrical in both principal axes, which introduces a dual-eccentricity of compression loading and weakens the column capacity furthermore.

Across the cored-hole location the column effective area is diminished. Additionally the unsymmetrical location of hole introduces eccentricity of axial loading applied on the cross section. The failure mode turned from axially compression to compression with small-eccentricity. The compressive stress flow in concrete is concentrated around the cored-hole, which causes premature compression capacity. It is therefore ascertained that the magnitude of capacity decline is depended on the location of core drilling, the dimensions of cross section, and whether core holes are repaired.

Column Ultimate Displacement It is also revealed by Table 2 that the ultimate displacement of the core-drilled columns experiences different scale of drop, which is altered between 1.88% and 26.14%. In contrast, the ultimate displacement of C6 increases 2.49%. The decline of ultimate displacement can be explained by the fact that an eccentric performance is developed by an unsymmetrical and less-effective-area cross section under axial loading.

Strain Distribution

Rebar Strain Distribution

The rebars have consistent strains under axial compression loading. After core drilling, the strains of longitudinal rebars at different side develop observable variations. Core-drilled column presents the growth of strains characterized by small-eccentricity loading. After repaired C6 reinstates consistent strains in longitudinal reinforcing rebars. The elaborated observation is verified by comparing the longitudinal rebar strains of C1 and C2 in Figure 8, and of C3~C6 in Figure 9.

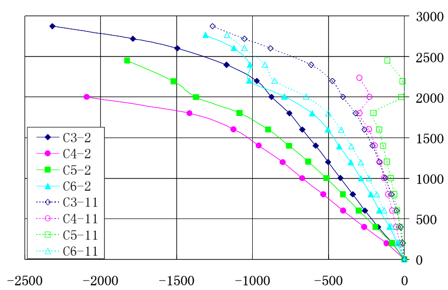

Figure 9: Rebar Strains of Specimens C3~C6

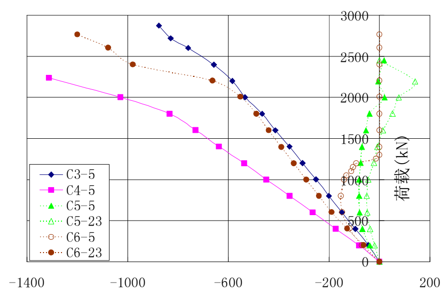

Figure 10: Rebar Strain at cored-hole positon

Although the center longitudinal reinforcing steel remaining continuous at the column side of C4, its strain is greater than the corresponding rebar of C3 at each level of loading. This strain enhance is evidently attributable to the cored-hole nearby the rebar on C4. C5 has the center longitudinal rebar discontinued by core drilling. The stress flow along the rebar is interrupted at the cored-hole and redistributed around. Therefore, the steel strain drops at the cutting end near the drilled hole. By repairing the drilled hole with concrete, the steel strain at the lower cutting end restores to a comparable level attained by C3 at corresponding loading. However, repairing the column at its vertical erection establishes discrete spaces between hole-filled concrete and the column. Thus, the steel strains achieved at the upper cutting end of rebar stay at equivalent magnitudes achieved by C5 at the corresponding location. The steel strains of C3~C6 are compared in Figure 10.

Concrete Strains Distribution

The concrete strains of C3~C6 are compared in Figure 11. It shall be pointed out that the specimens have equivalent concrete strains on each side of column at the condition of axial compression loading. After performed core drilling, the columns demonstrate apparent variations of the concrete strains on each side. This behavior is distinguished in columns subject to small-eccentricity compressions. After the core-drilled column is repaired, the concrete strains are re-established uniformly on each side of column as subject to axial loading.

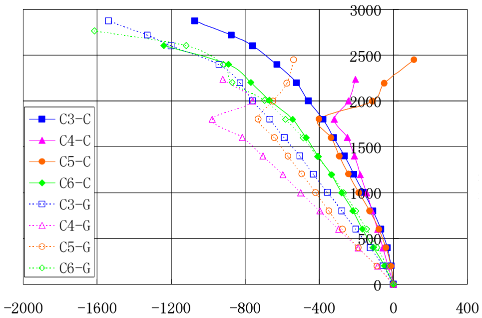

Figure 11: Concrete vertical strain of C3~C6

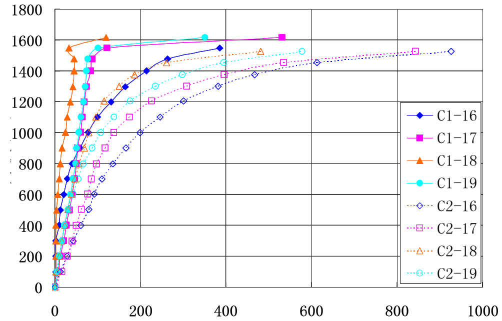

Figure 12: Striuup strain of C1~C2

Stirrup Strains Distribution

The stirrup steel strains of C1 and C2 are plot in Figure 12. As illustrated in Figure 12, the tensile strain of stirrups surrounding the drilled core is greater than those at the corresponding location of un-drilled specimen. This indicates that concrete confinement around the drilled hole is relied on adjacent stirrups.

Summary

Cored-holes will reduce the ultimate capacity of axial compression columns by 5.63% ~ 22.14% and the ultimate displacement by 1.88% ~ 26.14%.

Cored-holes will alter the behavior of columns subject to axial loading. The failure due to an axial compression is evolved into that due to small-eccentricity compression. The conversion of failure behaviors is also verified in the development of steel and concrete strains.

Repaired by slight-expansion high-strength concrete, impaired columns can achieve ultimate capacity with a decline of only 3.76% while improve ultimate displacement by 2.49%.

Cored-holes reduce the column effective section and redistributed stresses among concrete and rebar around the weakened section.

Acknowledgements

"The 11th-Five-Year Plan" National Key Technologies R&D Program (2006BAJ03A10-02) and Shanghai Science and Technology Commission Program (04-033) provided financial support to this research.

References

[1] Bartlett, M, and MacGregor, J (1994a). "Effect of moisture condition on concrete core strengths." *ACI Materials Journal*, 91(3), 227-236.

[2] Bartlett, M, and MacGregor, J (1994b). "Effect of core length-to-diameter ratio on concrete core strengths." *ACI Materials Journal*, 91(4), 339-348.

[3] Bartlett, M, and MacGregor, J (1994c). "Effect of core diameter on concrete core strengths." *ACI Materials Journal*, 91(5), 460-470.

[4] Bungey, J (1979). "Determining concrete strength by using small-diameter cores." *Magazine of Concrete Research*, 31(107), 91-98.

[5] CECS 03:88 (1988). Technical specification for testing concrete strength with drilled core.